Observations of earthquake source and ground motion scaling at the macro level

Paul G. Somerville[(1)]

(1) URS Corporation, 566 El Dorado Street, Pasadena, CA 91101, e-mail: paul_somerville@urscorp.com, phone 626 449-7650

Abstract

In this paper, we describe observational constraints on the scaling of earthquake source parameters. To first order, parameters such as rupture area, rise time, and the size and strength of asperities (regions of large slip) scale in a self-similar manner. The near fault rupture directivity pulse is a narrow band pulse whose period increases with magnitude. Current ground motion models, which all assume monotonically increasing spectral amplitude at all periods with increasing magnitude, do not provide an accurate description of near fault ground motions. The ground motions from buried faulting are consistently stronger than those from earthquakes having large surface slip.

Magnitude Scaling of Earthquake Source Parameters

The rupture models of 15 crustal earthquakes derived from the inversion of strong motion data were used by Somerville et al. (1999[6]) to develop magnitude scaling relations. These scaling relations, which are generally self-similar, are useful for characterizing earthquake rupture models for the prediction of strong ground motions. The source parameters include the fault rupture area, rise time averaged over the fault surface, and a set of parameters that describe the spatial variability of slip on the fault surface. These include the number, size and slip contrast of asperities, defined as regions having average slip that is 50% higher than the average fault slip. The scaling relations also include a wavenumber model for the spatial distribution of slip, which satisfies a K^{-2} wavenumber decay.

Magnitude Scaling of Response Spectra of the Forward Directivity Pulse

The propagation of fault rupture toward a site at a velocity close to the shear wave velocity causes most of the seismic energy from the rupture to arrive in a single large pulse of motion that occurs at the beginning of the record (Archuleta and Hartzell, 1984[3]; Somerville et al., 1997[7]). This pulse of motion represents the cumulative effect of almost all of the seismic radiation from the fault. The radiation pattern of the shear dislocation on the fault causes this large pulse of motion to be oriented in the direction perpendicular to the fault, causing the strike-normal ground motions to be larger than the strike-parallel ground motions at periods longer than about 0.5 seconds.

Strong motion recordings of the recent large earthquakes in Turkey and Taiwan confirm that the near fault pulse is a narrow band pulse whose period increases with magnitude (Figure 1). The recent earthquakes also have surprisingly weak ground motions at short and intermediate

periods (0.1 to 3.0 seconds), weaker than those of smaller (magnitude 6 ¾ - 7.0) earthquakes. These observations require reevaluation of the magnitude scaling in current models of near fault ground motions and in current source scaling relations (Somerville et al., 1999[6]).

On the left side of Figure 1, rupture directivity pulses of earthquakes in the magnitude range of 6.7 to 7 are compared with pulses from earthquakes in the magnitude range of 7.2 to 7.6. The narrow band nature of these pulses causes their elastic response spectra to have peaks, as shown on the right side of Figure 1. The fault normal components (which contain the directivity pulse) are shown as solid lines, and the fault parallel components, which as expected are much smaller at long periods, are shown by long dashed lines. The 1994 UBC spectrum for soil site conditions is used as a reference model for comparison.

The spectra for the large earthquakes (right column) are compatible with the UBC code spectrum in the intermediate period range, between 0.5 and 2.5 seconds, but have a bump at a period of about 4 seconds where they significantly exceed the UBC code spectrum. The spectra of the smaller earthquakes (left column) are very different from those of the larger earthquakes. Their spectra are much larger than the UBC code spectrum in the intermediate period range of 0.5 - 2.5 sec, but are similar to the UBC spectrum at longer periods. The magnitude scaling exhibited in the data in Figure 1 is contrary to all current models of earthquake source spectral scaling and ground motion spectral scaling with magnitude, including Somerville et al. (1997[7]), which assume that spectral amplitudes increase monotonically with magnitude at all periods. However, these magnitude scaling features are the natural consequence of the narrow band character of the forward rupture directivity pulse.

Relationship between Magnitude and the Period of the Forward Directivity Pulse

In Figure 2, we show a relationship between the period of the pulse and earthquake magnitude M_w that includes data from the 1999 Turkey and Taiwan earthquakes. This relationship uses the period of the largest cycle of the fault normal velocity waveform recorded at stations near the fault that experience forward rupture directivity. The recordings used are within 10 km of the fault, and the period is assumed to be independent of the distance from the fault. The data are consistent with a self-similar scaling relationship in which the period of the pulse T_p increases in proportion to the fault length:

$$\text{Log}_{10} T_p = -3.1 + 0.5 M_w$$

Alavi and Krawinkler (2000[2]) proposed that equations like this can be directly used in the design of structures to withstand near fault ground motions, using simple pulse representations of near fault ground motions.

Ground Motions from Surface and Subsurface Faulting

The rupture of the 1989 Loma Prieta and 1994 Northridge earthquakes stopped at depths of several km below the surface. Although there was some surface faulting on Awaji Island during the 1995 Kobe earthquake, the strong motion recordings of the Kobe event were dominated by subsurface faulting on the Suwa and Sumayama faults. Thus all of the earthquakes in the magnitude range of 6.7 – 7.0 shown in Figure 1 are characterized by subsurface faulting, while all of the earthquakes in the magnitude range of 7.2 to 7.6 are

characterized by large amounts of surface faulting. Consequently, some of the differences seen in these figures may be attributable not only to magnitude effects, but to the effects of buried faulting. Indeed, at short and intermediate periods, the ground motions from earthquakes that produce large surface rupture appear to be systematically weaker than those whose rupture is confined to the subsurface, although current empirical ground motion models do not distinguish between these different categories of earthquakes.

This is indicated in Figure 3, which shows the residuals between the ground motions of selected individual earthquakes, averaged over recording stations, and the empirical ground motion model of Abrahamson and Silva (1997[1]) for surface rupture earthquakes (top and center) and subsurface rupture earthquakes (bottom). The zero line represents the Abrahamson and Silva (1997[1]) model, which takes account of magnitude, distance, and site conditions, and lines above the zero line indicate an event exceeding the model. At periods shorter than 3 seconds, the ground motions from earthquakes that produce large surface rupture are significantly weaker that those in which rupture is confined to the subsurface.

These observations about strong ground motions have important implications for dynamic rupture models of earthquakes. For example, the difference in ground motions between subsurface and surface faulting may be related to a slip weakening phenomenon that causes a transition from confined rupture to "runaway" rupture (Kanamori and Heaton, 2000[5]). The mechanism for such slip weakening phenomena may be related to elastohydrodynamic lubrication (Brodsky and Kanamori, 2000[4]).

References

[1] Abrahamson. N.A. and W.J. Silva (1997). *Empirical response spectral attenuation relations for shallow crustal earthquakes*, Seismological Research Letters 68, 94-127.

[2] Alavi, B. and H. Krawinkler (2000). *Design considerations for near-fault ground motions.* Proceedings of the U.S. – Japan Workshop on the Effects of Near-Fault Earthquake Shaking, San Francisco, March 20-21.

[3] Archuleta, R. J. and S. H. Hartzell (1981). *Effects of fault finiteness on near-source ground motion*, Bull. Seism. Soc. Am. **71**, 939-957.

[4] Brodsky, E. and H. Kanamori (2000). *The elastohydrodynamic lubrication of faults*. Unpublished manuscript.

[5] Kanamori, H. and T.H. Heaton (2000). *Microscopic and macroscopic physics of earthquakes*. AGU Monograph, in press.

[6] Somerville, P.G., K. Irikura, R, Graves, S. Sawada, D. Wald, N. Abrahamson, Y. Iwasaki, T. Kagawa, N. Smith and A. Kowada (1999). *Characterizing crustal earthquake slip models for the prediction of strong ground motion*. Seism. Res. Lett. 70, 59-80.

[7] Somerville, P.G., N.F. Smith, R.W. Graves, and N.A. Abrahamson (1997). *Modification of empirical strong ground motion attenuation relations to include the amplitude and duration effects of rupture directivity*, Seismological Research Letters 68, 199-222.

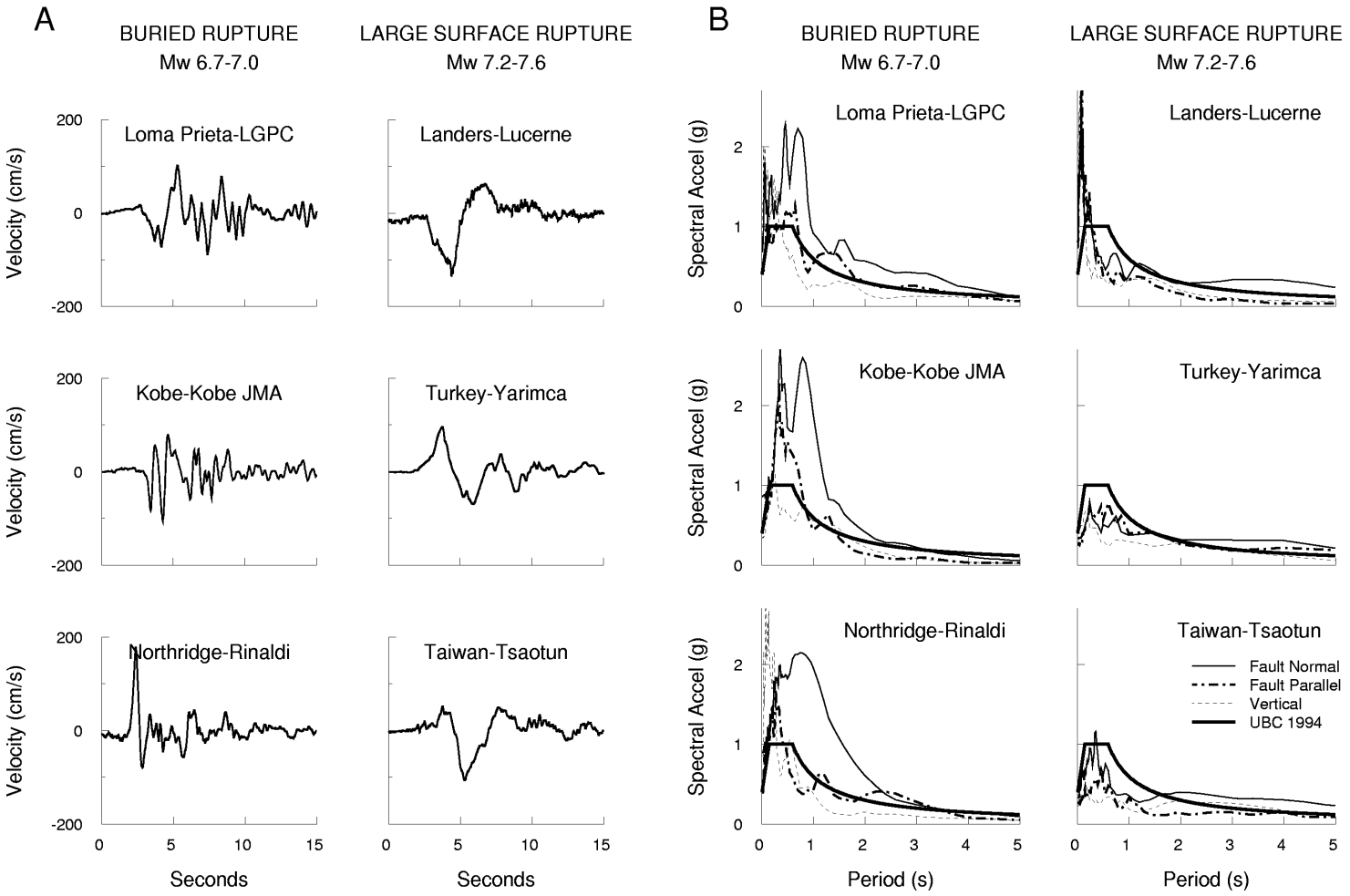

Figure 1. A: Fault-normal velocity pulses recorded near three moderate magnitude earthquakes (left column) and three large magnitude earthquakes (right column), shown on the same scales. B: Corresponding acceleration response spectra, with 1994 UBC code spectrum shown for reference.

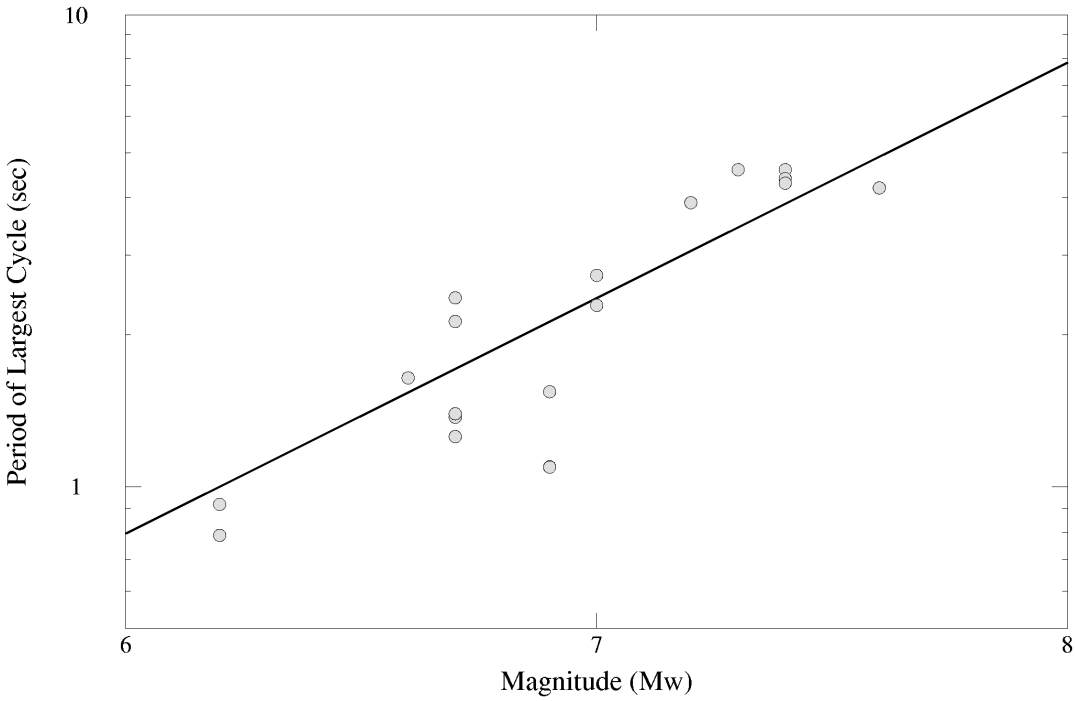

Figure 2. Relation between period of fault normal pulse and Mw for forward directivity